TECHNOLOGY DIGEST
TD-10-004
©MARCH 2010
TIMELY TECHNOLOGY TRANSFER

The work described in this document was performed by Transportation Technology Center, Inc.,
a wholly owned subsidiary of the Association of American Railroads.

Shell Defect Analysis Using Scanning Electron Microscopy Techniques

Daniel Szablewski and Francisco C. Robles Hernández (University of Houston)

Summary

A number of shell defects develop on the high rail gage side in 5 and 6-degree curves, as well as in spirals leading into them, in the High Tonnage Loop (HTL) at the Facility for Accelerated Service Testing (FAST), Pueblo, Colorado. The rate of shell development is accelerated compared to what would be expected in revenue service. For instance, in 5 months (January-May 2008), Transportation Technology Center, Inc. engineers identified 11 weld shell defects in spirals, and 55 weld shell defects in curves in the HTL.[1] Reported here is an insight into the analysis of the primary root cause(s) of shell defects.

The Scanning Electron Microscopy analysis performed as part of this investigation yields the following conclusions:

- Rail shell defects in the HTL originate as cracks in the subsurface of the high rail gage corner 1/4 to 3/8 inch from the gage corner surface in 5- and 6-degree curves at FAST. These cracks propagate in a plane parallel to the gage corner surface outward in all directions until they reach the head surface, at which point shell separation from the bulk of the railhead takes place.
- Although many of the shell fracture surfaces were severely damaged during their formation process, counting the fracture surface saw tooth marks and relating that information to the changes in the train travel direction. The MGT accumulated by the rail during that time reveals that in 39-ton axle load environment this type of shell formation takes 20-40 MGT from initiation to critical failure.
- The shell growth direction is dependent on the direction of train operation, and it is controlled by the shear stress field in the railhead.
- The shelled fracture surface morphologies display marks characteristic of fatigue crack growth and failure.
- Due to the extreme forces at work during the fatigue crack growth, the cracked surfaces are destroyed during shell formation. As a result, most of the evidence of crack history is erased during crack propagation in the railhead, which makes determining the root causes of shelling with certainty rather difficult.
- However, there is evidence of soft (MnS), hard (Al_2O_3), and complex oxide inclusions in the ridges of the fatigue marks on the shelled surfaces. These inclusions range in size from 50-100 μm. It is very likely that these inclusions contributed to the formation of the shells.

A recommendation to eliminate shells in curved track would be to produce cleaner steel rails with reduced amount of inclusions, in order to reduce the amount of stress risers in the high shear stress field located in the high railhead gage corner in curves.

This investigation raises the awareness of rail steel cleanliness and its affect on the formation of deep seated shells. Future work will focus on a thorough investigation of the link between rail microcleanliness and shell formation.

The Association of American Railroads' Strategic Research Initiatives Program provided funding for this research.

Please contact **Daniel Szablewski (719) 585-1852** with questions or concerns regarding this *Technology Digest.* E-mail: daniel_szablewski@ttci.aar.com.

BACKGROUND

The development and implementation of premium rail steels over the years has been very successful, yielding a noticeable in-service rail life extension. The main improvement has been in wear resistance of the railhead. This was achieved by making the railhead harder and targeting a fully pearlitic railhead microstructure, both realized through advances in rail chemistry, thermo-mechanical processing (TMP), and cooling practices.

Nowadays, major North American Class I railroads use premium rails in curves having more than 2 degrees of curvature and in tangent track with traffic in excess of 60 MGT/year.[2] A 2008 rail life investigation by TTCI determined that wear is still the primary mode of rail degradation and that the percentage of rail replacement increases with track curvature due to wear.[3] In particular, a study of three commercial freight railroads revealed that wear-related rail removal is in excess of 80 percent for track curvature above 2 degrees. Rail breaks, weld breaks, rolling contact fatigue (RCF), and rail shell defects are still significant causes for rail replacement. However, rail failure due to these reasons usually occurs in track with less than 2 degrees of curvature.[3] Results from another TTCI study reported that a major contributor to fatigue related failures is the presence of inclusion defects in the steel microstructure.[4]

There are two identifiable groups of inclusions that can form in steel during the manufacturing process. The first group is referred to as exogenous inclusions, which enter the liquid steel either as a result of the erosion of refractories or are formed as a result of slag particle entrapment. These are mostly large-sized inclusions with complex structures and irregular shapes. Premium rail manufacturers use nondestructive testing (NDT) systems to monitor the rail to detect such large discontinuities. Premium rails are thoroughly inspected by the manufacturers before they are sold. The entire rail is scanned prior to delivery to the customer to guarantee that exogenous inclusions do not exist in the rail.

The second group of inclusions is referred to as indigenous inclusions. These types of inclusions form due to the physical chemistry of steelmaking and are a result of the chemical reactions that take place in either liquid or solid state steel.[5] These inclusions are very small and, as a result, are beyond the detection limits of standard NDT test methods.

The inclusions analyzed in this investigation were the indigenous inclusions. A thorough review of indigenous inclusions groups them into a number of categories based on their severity of impact on the mechanical properties.[5] The most detrimental group was identified as clusters of small particles, referred to as either “galaxies” or “picket fence” arrangements. Al_2O_3 and MnS fall into those respective categories. In as-cast billet form, the behavior of the inclusion cluster is difficult to predict, because they have no particular preferred orientation. However, the hot rolling of rail causes the clusters to deform preferentially along the rolling direction. This is an important consideration because the deep seated shells open up primarily in the rail rolling direction, which is also the major plane of the rolled inclusions, as well as the plane on which the shear forces in the rail act. This combination of favorable conditions for shell formation has an important role in their occurrence.

With the past explorations of conventional methods to design new pearlitic rail steels (e.g., alloying), there is limited room left for incremental improvements. However, TTCI in collaboration with the University of Pittsburgh developed a next-generation rail steel chemistry, combined with advanced TMP and cooling practices, that offers substantial improvements in mechanical performance and a reduced inclusion content.[6,7] This rail steel is expected to exhibit improved in-track performance by diminishing the occurrence of fatigue failures (e.g., RCF, and deep-seated shelling).

Operations on the High Tonnage Loop

The HTL at FAST is a 2.7-mile-long closed loop track. Curves make up 54 percent of the track: 34 percent of the track is composed of three 5-degree curves, and 20 percent of the track is covered by a single 6-degree curve. Spirals that lead into and out of curves make up 11 percent of the entire track length. The rest of the track (35%) consists of tangent track, which results in a disproportionate amount of curving (54% of track is curves) during train operation and influences the accelerated wear behavior of the rails and subsequent shell development when the rail wears out. All the shells collected originated on the gage side corner of the high rail. In 5 months (January-May 2008), TTCI identified 11 weld shell defects in spirals, 55 weld shell defects in curves, and 6 weld shell defects in tangent track.[1]

TTCI operates a HAL train on the HTL made up of 39-ton axle load cars. An accumulated tonnage of approximately 1.3-1.6 MGT is commonly achieved during each night of train operation. The traffic on the HTL is bi-directional with approximately 50 percent of traffic in each direction. Once the shell is initiated, the fatigue crack growth is controlled by the shear stress field. As a result, the cracks grow preferentially in the direction of train travel. The formed cracks have the opportunity to grow radially in all directions, eventually leading to critical failure.

TTCI uses an automated, conventional ultrasonic rail flaw detection system to inspect the rails on a regular basis. However, a number of the defects were detected through visual inspection. This was particularly true for the rail shell defects, which are difficult to pick up using the conventional rail flaw detection system.

Rail Shell Sample Selection from FAST

In order to investigate the root cause of these shell defects, a selected number of representative weld and rail shell defects were extracted from the track and prepared for Scanning Electron Microscopy (SEM) analysis. Table 1 lists the samples extracted from the HTL for this analysis. Table 1 does not represent the proportionate distribution of all the shells that exist at FAST, but only the shells that were available for analysis at the time the investigation was conducted.

Table 1. Summary of railhead samples that exhibited shelling in the high rail gage corner. Samples 1, 6, 9, and 10 were analyzed in the SEM

No.	Defect Origin	Rail Type	Hardness	Lub. Condition	MGT Accum.
1	Head Repair Weld	136 RE - ERMS DHH	~370 HB	Lub. Carryover	~150 MGT
2	Head Repair Weld	136 RE - ERMS DHH	~370 HB	Lub. Carryover	~125 MGT
3	Orgo-Therm. Weld	136 RE - ERMS DHH	~370 HB	Lub. Carryover	~150 MGT
4	Rail	141 RE - VA HHC	~400 HB	Not Lubricated	~500 MGT
5	Rail	136 RE - NKK HE	~380 HB	Direct Lub.	~250 MGT
6	Rail	136 RE - NKK HE	~380 HB	Direct Lub.	~250 MGT
7	Rail	141 RE - ERMS HCP	~395 HB	Direct Lub.	~760 MGT
8	Rail	141 RE - ERMS HCP	~395 HB	Direct Lub.	~760 MGT
9	Rail	141 RE - ERMS HCP	~395 HB	Direct Lub.	~760 MGT
10	Rail	141 RE - ERMS HCP	~395 HB	Direct Lub.	~760 MGT
11	Rail	141 RE - VA HHC	~400 HB	Not Lubricated	~500 MGT

As Table 1 indicates, the samples represent a range of rail profiles, head hardnesses, and lubrication conditions. In particular, samples 1-3 represent weld defects originated in section 31 of the HTL. This is a 5-degree curve that is ground but is not directly lubricated. However, there is a limited amount of lubrication carryover from adjacent section. The head hardness of the rail in this curve is ~370 HB. Samples 4 and 11 represent rail shell defects extracted from section 7. This section is a 5-degree curve used for wear testing of a variety of premium rail grades. At the time of the shell formation, lubrication was not used in this section. The hardness of these rails is ~400 HB, and the section of the curve where these two shells were found was not ground. Samples 5 and 6 are rail shells taken from section 26, which is a spiral section that is not ground, but lubricated. Whereas, samples 7-10 are rail shells taken from section 25, which is a 6-degree curve that is directly lubricated. Section 25 had a rail grinding trial on the premium rails.[8] However, the extracted shells came from the unground section of the curve that was used as a baseline for the grinding experiment. Not all of the shells could be analyzed under the SEM due to the damage that some of the shells sustained during train operation. Four shells with the least amount of damage were selected for analysis in the SEM. They are shells 1, 6, 9, and 10.

Correlation of lubrication to the MGT accumulated by the rail prior to shelling clearly indicates that even though section 25 is a 6-degree curve, the MGT accumulated prior to shelling was approximately 760 MGT (the highest of all shelled rails investigated).

Shell 1 was extracted from the high rail of a 5-degree curve, shell 6 from the high rail of a spiral, and shells 9 and 10 were extracted from the high rail of a 6-degree curve. All defects analyzed originated on the gage side of the high rail.

Sample Preparation and Testing Methodology

Three head-weld shells and eight rail shells were removed from the HTL using saw cutting. Figure 1 is a schematic showing the location of a typical rail shell defect in reference to the wheel; whereas the example of an actual rail shell (bottom photo) removed from the railhead (top photo) on the HTL is shown in Figure 2.

A survey of all the shell defects found on the HTL indicates that the rail shells originate as cracks in the subsurface of the high rail gage corner 1/4 to 3/8 inches from the gage corner surface of the rail, as Figure 1 illustrates. The cracks propagate in a plane parallel to the gage surface of the rail outward in all directions until they reach the head surface, resulting in shell separation from the railhead. In the cases investigated here, complete shell separation from the railhead did not take place. As a result, the shells had to be cut out of the rail using a band saw.

Scanning Electron Microscopy Analysis

The SEM samples were vacuum carbon coated using an evaporation method to improve sample conductivity and SEM image quality. They were then placed under vacuum in the JEOL JSM-633OF Field Emission Scanning Electron Microscope. The microscope was operated at 15kV accelerating voltage. The imaging used included Secondary Imaging and Backscatter Imaging with Electron Dispersive Spectroscopy (EDS). EDS technique was used to determine the chemical composition of the inclusions.

Although many of the shell fracture surfaces were severely damaged during their formation, the shell fracture growth rings (also referred to as saw tooth topology) are clearly visible on each fracture surface (see Figure 2). The characteristic steps in these saw tooth marks have previously been associated with the changes in the direction of train travel.[9] Counting these saw tooth marks and relating that information to the number of nights the test train at FAST runs in each direction and combining that information with the MGT accumulated by the rails during that time indicates that the shell formation takes 20-40 MGT from initiation to final fracture.[10]

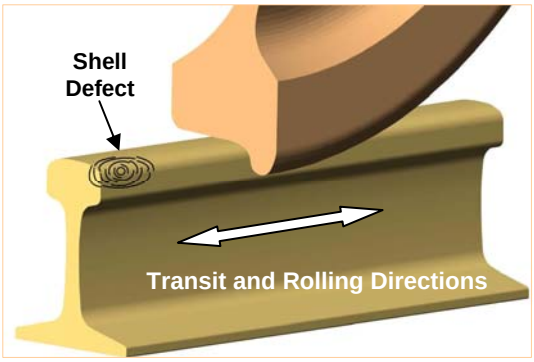

Figure 1. Schematic of a shell defect formed in the head region on the gage side of the railhead at FAST-HTL

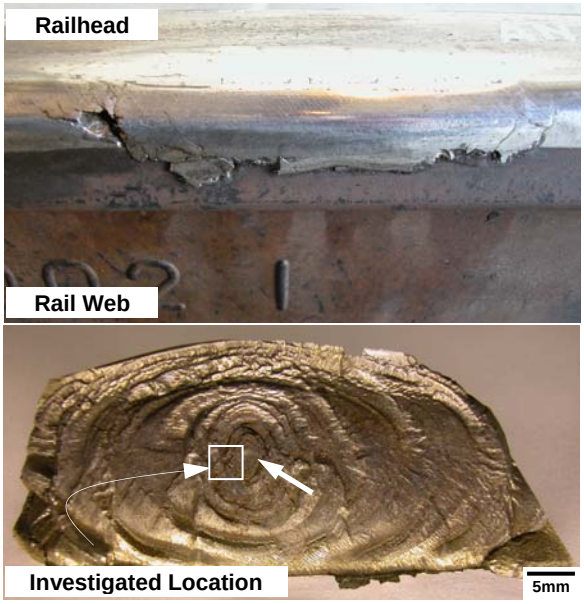

Figure 2. Rail shell defect as observed in the Railhead, and post-removal from railhead, SEM analysis location indicated.

When imaging the investigated locations, the work focused on identifying the presence of inclusions at the shelled surfaces. In many instances, little was found. This was due to the failure mechanism. The forces with which the newly formed shell surfaces impact and rub against each other during train operation contributes to their growth. However, this action also destroys the fracture surfaces, erasing a major part of the fracture history. This makes pinpointing the root cause of the shell with all certainty rather difficult. The limited evidence that remains is hidden in the ridges of the shelled surfaces. The SEM analysis conducted focused on these ridges in an effort to pinpoint the type of inclusions and their morphology.

The inclusions that had a predominant presence in all the shells investigated were Al2O3, complex oxides and MnS. The observed inclusions ranged in size from 50 µm to 100 µm. They were located mainly in the ridges of the saw tooth marks, probably because of their stability in this location of the shelled surface. They were, however, severely damaged as Figure 3 indicates. Of particular interest is the clear evidence of cleavage (brittle fracture) that is initiated by the presence of the inclusions shown in Figure 3 (top photo). It is very likely that these types of inclusions contributed to the formation of the shell defects.

Figure 4 shows an EDS spectra attained for a soft (MnS), hard (Al_2O_3) and complex oxide inclusions, respectively. Mn and S peaks can be clearly distinguished. The presence of K, Cl, O in the inclusion is an indication of a complex oxide inclusion. Other labeled peaks indicate the neighboring steel matrix structure.

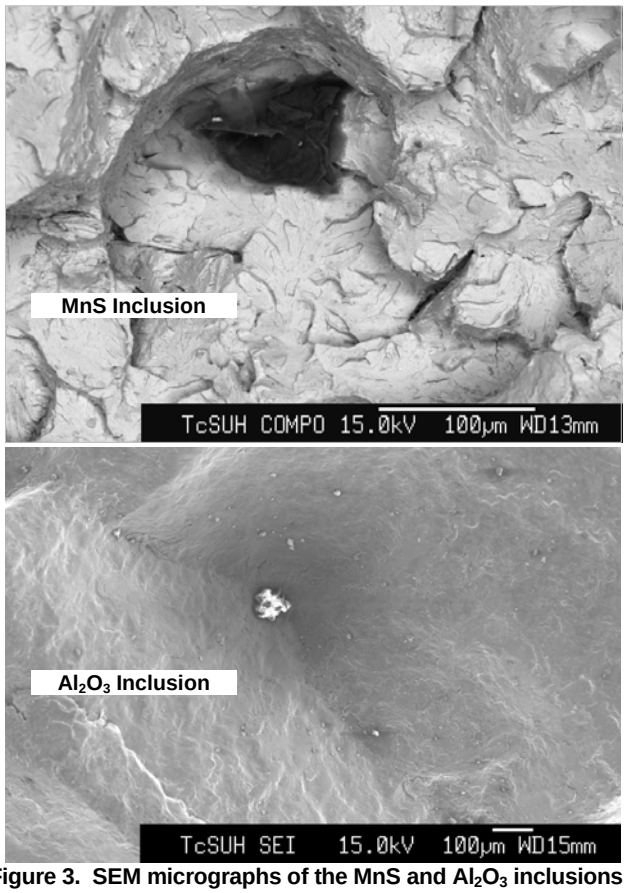

Figure 3. SEM micrographs of the MnS and Al_2O_3 inclusions present in the ridges of the shelled surface

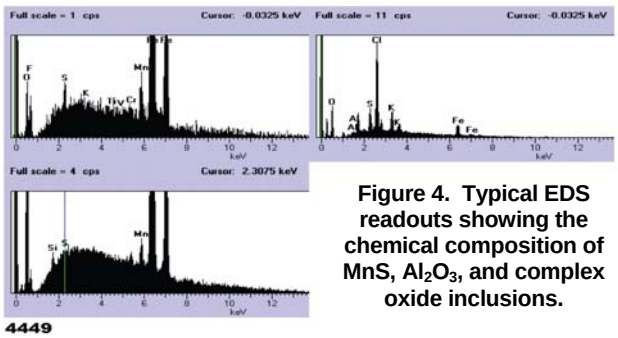

Figure 4. Typical EDS readouts showing the chemical composition of MnS, Al_2O_3, and complex oxide inclusions.

CONCLUSIONS

The main reason for premature rail removal is mainly related to fatigue issues, among which shelling is significant. Revenue service data for 2008 indicates that the amount of rail removed due to breaks, RCF, and other defect types is a concern. The amount of money spent on rail repair continues to be a major part of annual railroad track maintenance budgets. As a result, an effort is needed towards developing rails that are less prone to failure due to fatigue.

A SEM investigation of the deep seated shells indicates that there is a presence of MnS, Al_2O_3, and complex oxide inclusions in the ridges of the fatigue saw tooth marks close to the shell initiation locations. It is very likely that these inclusions contributed to the formation of shell defects. The propagation of the shells observed was parallel to the rolling surface on the high rail gage corner. The growth direction was preferential depending on the direction of train operation, and it was controlled by the shear stress field in the railhead.

A recommendation to eliminate shells in curved track would be to produce rails with reduced amount of inclusions, in order to reduce the amount of stress risers in the high shear stress field located in the high rail gage corner of the railhead.

Acknowledgements

Special appreciation to TTCI employees Ira Kalb, Greg Giebel, and Ken Trujillo for the extraction and preparation of the rail shell samples, and to Satima Anankitpaiboon for preparing the illustrative sketch.

References

1. Kalb I., G. Giebel, and K. Trujillo. 2008. TTCI In-house yearly log: Rail Defect Monitoring, not for distribution.
2. BNSF Railway. October 2007. Class I Railroad Engineering Instructions, 6 Rail. p. 6-7.
3. Pinney C. 2008. TTCI In-house documentation: Rail Life Study, not for distribution.
4. Robles Hernandez F. C., and J. LoPresti. March 2009. "Linking Fatigue, Microcleanliness, Tensile, and Fracture Toughness Tests," *Technology Digest*, TD-09-010, AAR, TTCI, Pueblo, CO.
5. DeArdo A. J. 1986. *Encyclopedia of Materials Science and Engineering–Inclusion Control in Steel*, p. 2275-2279, Pergamon Press.
6. Ordóñez Olivares, R. A. et al. August 2009. "New Rail Steels for the 21st Century: Superior Performance through Advanced Alloy Design and Thermo-Mechanical Processing," Limited Availability LA-033, Full members railroads only.
7. Ordóñez Olivares, R., et al. April 2009. "New Rail Steel for the 21st Century: Advanced Alloy Thermo-Mechanical Processing Development," *Technology Digest*, TD-09-011, AAR, TTCI, Pueblo, CO.
8. LoPresti J. October 2007. "Effects of Rail Profile Grinding on High-Hardness Premium Rail at FAST," *Technology Digest*, TD-07-032, AAR, TTCI, Pueblo, CO.
9. Stone D. H. 2000. "Shattered Rim Defects in Wheels," IMechE Seminar Publication 2000-20, Wheels and Axles Cost-effective Engineering.
10. Fec M. C. 1985. "Elevated Temperature Fatigue Behavior Of Class B, C, and U Wheel Steels," *ASME – Rail Transportation Spring Conference Proceedings.*